



HAL
open science

Fluorescence Commutation and Surface Photopatterning with Porphyrin Tetradithienylethene Switches

Thomas Biellmann, Agostino Galanti, Julien Boixel, Jennifer A. Wytko,
Véronique Guerchais, Paolo Samori, Jean Weiss

► **To cite this version:**

Thomas Biellmann, Agostino Galanti, Julien Boixel, Jennifer A. Wytko, Véronique Guerchais, et al.. Fluorescence Commutation and Surface Photopatterning with Porphyrin Tetradithienylethene Switches. *Chemistry - A European Journal*, 2018, 24 (7), pp.1631-1639. 10.1002/chem.201704222 . hal-01709536

HAL Id: hal-01709536

<https://univ-rennes.hal.science/hal-01709536>

Submitted on 28 Feb 2018

HAL is a multi-disciplinary open access archive for the deposit and dissemination of scientific research documents, whether they are published or not. The documents may come from teaching and research institutions in France or abroad, or from public or private research centers.

L'archive ouverte pluridisciplinaire **HAL**, est destinée au dépôt et à la diffusion de documents scientifiques de niveau recherche, publiés ou non, émanant des établissements d'enseignement et de recherche français ou étrangers, des laboratoires publics ou privés.

Fluorescence commutation and surface photopatterning with porphyrin tetra-dithienylethene switches

Thomas Biellmann,^[a] Agostino Galanti,^[b] Julien Boixel,^[c] Jennifer A. Wytko,^[a] Véronique Guerchais*^[c] Paolo Samori*^[b] and Jean Weiss*^[a]

Abstract: Four tetra-dithienylethene (DTE) substituted porphyrins, the free base **1H₂** and three metal derivatives (**1Zn**, **1Co**, **1Ni**), were synthesized and studied. These dyads, in which the DTE units are connected to the porphyrin's meso positions via a *meta*-phenyl spacer, exhibit reversible photochromic properties in all cases with conversion to the PSS up to 88%, as confirmed by absorption and NMR spectroscopies. Compounds **1H₂** and **1Zn** are fluorescent in solution and display a red emission. Upon irradiation with UV light to trigger the closing of the DTEs, the fluorescence of both the free base and zinc porphyrin was very efficiently quenched in solution. The reversible, photo-triggered switching of luminescence was retained in a tetra-DTE free base porphyrin-doped polystyrene film, for which photo-patterning was demonstrated by confocal scanning microscopy. The tunable fluorescent properties of this multi-DTE framework render this compound of interest as a photo-rewritable fluorescent ink.

Introduction

Among the known photochromic switches,^[1] the dithienylethene (DTE) scaffold is particularly attractive because of its efficient, fast and fatigue-resistant photoisomerization combined with its thermodynamic stability in both the *open* and *closed* isomers.^[2] Based on these features, the potential of DTEs as components in photo-electronic devices is now well established,^[3] as is their capability of controlling a variety of properties when incorporated in molecular architectures.^[4-9] By increasing the number of photoswitches in a single component, one could potentially increase the contrast in the photoresponse of the system, rendering such compounds appealing for information storage.^[10] A major challenge in the development of novel, functional systems addressable with light stimuli is therefore to integrate as many efficient photoswitchable units as possible in the same molecular backbone. In multi-photochromic systems in general, and more particularly in multi-DTE scaffolds, the photoresponse was found to depend on reciprocal electronic interactions between the DTE

moieties. In many cases, complete closure of the DTEs does not occur because, upon UV irradiation of a scaffold containing both *open* and *closed* DTE moieties, intramolecular energy transfer from an *open* to a *closed* DTE may prevent additional ring closures. Although exceptionally high *closed* to *open* ratios (>90%) were reported for di-,^[11,12] tri-^[12] and hexa-DTE^[13] arrays, most multi-DTE scaffolds exhibited more modest photoisomerization results.^[14-17]

Extensive investigations on multi-photochromic molecular systems have helped to elucidate the role of the bridging unit interconnecting the chromophores within the same molecular scaffold.^[14] Photochromism inhibition typically results upon conjugation of the photoswitch with an extended aromatic system due to the appearance of a low-lying excited state that does not lead to the desired photoisomerization. Generally, suitable connectors must be chosen to decrease the electronic delocalization over the entire π -backbone. Although diverse linkers^[11,14,17-21] have been incorporated into multi-DTE molecular architectures, porphyrins are rarely employed as bridges despite their robustness, symmetry and unique opto-electronic properties. Examples of porphyrins bearing two^[22] or four^[23] azobenzene switches with contrasting photoisomerization capabilities were reported; yet, to date, the only multi-DTE mono-porphyrin scaffolds are a tin(IV) porphyrin with two axially coordinated phenoxide-DTEs^[24] and an azaporphyrin with bithienylethenes incorporated across the beta-positions of all four pyrroles.^[16]

The combination of DTEs with porphyrins is an appealing way to modulate light-triggered intra- or intermolecular processes, such as electron^[25-26] or energy^[27] transfer or singlet oxygen generation.^[28] Moreover, photochromic compounds displaying reversible fluorescence switching properties are of great interest in the field of superresolution fluorescence microscopy, for the fabrication of rewritable fluorescent photoinks.^[12] or as phototriggered fluorescent probes.^[29-31]

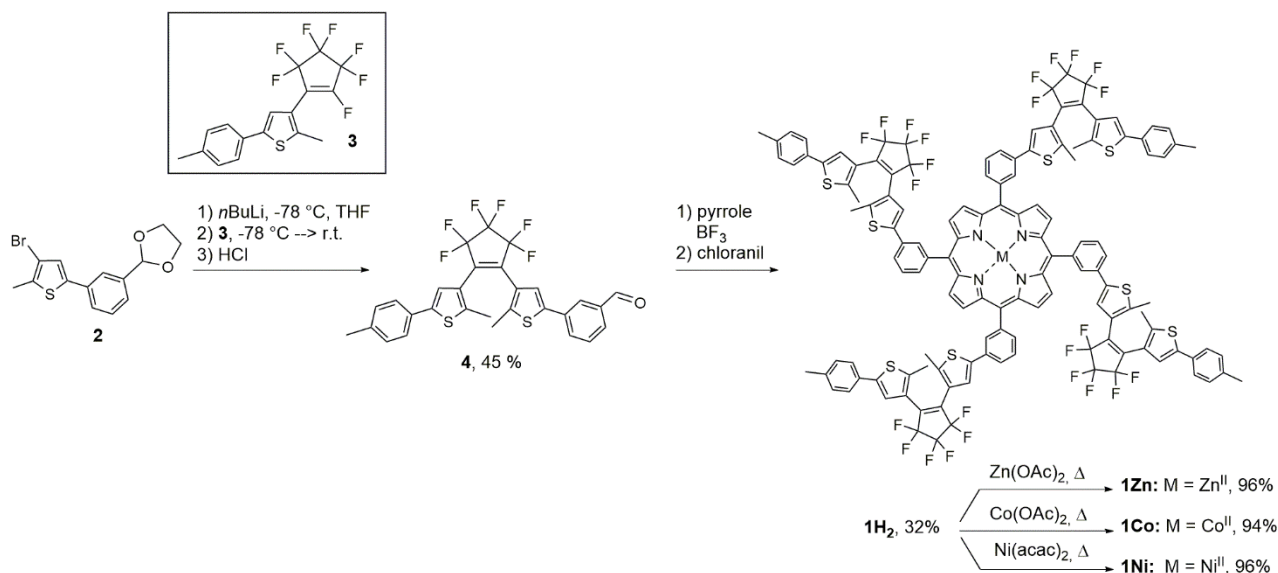
Porphyrins luminesce intensely in the red part of the visible light spectrum where the *open* DTE isomer does not absorb. Moreover, porphyrin emission occurs upon excitation with visible light, at wavelengths at which DTE photochromism is not triggered. Thus, readout by fluorimetry can occur at a wavelength far from that required for photoisomerization, in the UV region. In addition, spectral overlap of the *closed* DTE's absorption in the visible region with the emission band of the porphyrin provides a means of regulating their luminescence, as demonstrated by quenching of the emission upon photoisomerization.^[24,26,32-34] Porphyrins also offer a possible large energy difference between the excitation and emission wavelengths, e.g. by excitation of the Soret band ca. 420 nm and emission at 650 nm; this difference exceeds the normal Stokes shift when excitation occurs in the Q band. This large shift facilitates detection of the emission and avoids scattering from the excitation light, thus opening the door to applications as "rewritable fluorescent photoinks."

[a] Dr. T. Biellmann, Dr. J. A. Wytko, Dr. J. Weiss
Institut de Chimie de Strasbourg
UMR 7177 CNRS-Université de Strasbourg
4 rue Blaise Pascal, F-67000 Strasbourg, France
E-mail: jweiss@unistra.fr

[b] Mr. A. Galanti, Prof. P. Samori
University of Strasbourg, CNRS, ISIS UMR 7006,
8 allée Gaspard Monge, F-67000 Strasbourg, France
E-mail: samori@unistra.fr

[c] Dr. J. Boixel, Dr. V. Guerchais
Institut des Sciences Chimiques de Rennes
UMR 6226 CNRS – Université de Rennes 1
263 avenue du Général Leclerc, 35042 Rennes Cedex, France
E-mail: veronique.guerchais@univ-rennes1.fr

Supporting information for this article is given via a link at the end of the document.



Scheme 1. Synthesis of free base and metallated tetra-DTE porphyrins.

With the aim of designing molecular switches with high contrast, an emissive porphyrin was used as a symmetric framework for four DTE units. Thus, we synthesized four photoswitchable compounds (Scheme 1), namely the free base **1H₂** and the corresponding metal derivatives (**1Zn**, **1Co**, **1Ni**). The free base and zinc derivatives should ensure efficient luminescence commutation. The four DTE units were incorporated at the *meta* position of a tetraphenylporphyrin core not only to avoid the formation of atropisomers, but also to limit electronic communication between the porphyrin ring and the DTEs. Reduced electronic communication between the porphyrin and the DTE chromophores should preserve the photochromic behavior of the DTE units. The photochromic properties of these scaffolds were monitored by ¹H NMR, UV-visible absorption and emission spectroscopies. Furthermore, using confocal laser scanning microscopy, photopatterning of fluorescence was also demonstrated for bi-component films of **1H₂** embedded in a polystyrene matrix.

Results and Discussion

Synthesis

The synthesis of the tetra-DTE metal-free porphyrin **1H₂** was achieved in 32% yield by Lewis acid catalyzed condensation^[35] of the DTE-based aldehyde **4** with pyrrole and subsequent oxidation with *p*-chloranil (Scheme 1). The unsymmetrically substituted DTE **4** was prepared by a reported procedure^[5b] from the 4-bromothiophene derivative **2**^[36] bearing a protected benzaldehyde and the perfluorocyclopentene derivative **3**,^[37] followed by deprotection of the aldehyde under acidic conditions. An inert tolyl substituent was chosen for the end of the DTE arms to facilitate characterization by ¹H NMR during photoisomerization experiments. Metalloporphyrins **1Zn**, **1Co** and **1Ni** were prepared in excellent yields by reaction of **1H₂** with the corresponding metal salt, i.e., $\text{Zn}(\text{OAc})_2$, $\text{Co}(\text{OAc})_2$ and $\text{Ni}(\text{acac})_2$ respectively.

Except for the paramagnetic **1Co**, compounds **1H₂**, **1Ni** and **1Zn** were characterized by ¹H NMR spectroscopy (CD_2Cl_2). The presence of a single peak for the beta-pyrrolic protons near 9 ppm confirms the four-fold symmetry of the molecules. Typically, the

spectrum of **1H₂** (Figure 1, bottom) exhibits two singlets at δ 7.46 and δ 7.18 ppm, assigned to the magnetically non-equivalent thienyl protons of the four DTE units in their *open* forms, whereas the protons of the methyl groups appear as one broad signal at δ 1.95 ppm. The ¹H NMR spectra of metal-based porphyrins **1Zn** and **1Ni** display similar NMR features for the DTE protons.

The electronic absorption spectrum of each tetra-DTE-porphyrin array shows the typical features of the two chromophores, with a broad band in the UV region attributed to the π - π^* transitions of the *open*-DTE in addition to the porphyrin's characteristic Soret and Q bands in the visible region (Table 1 and ESI). Four Q bands are observed for **1H₂** at 517, 551, 590 and 646 nm (Figure 2, Table 1 and ESI). Fewer (two or one) Q bands are observed for the metallated porphyrins **1Zn** (Figure 2 and ESI), **1Ni** and **1Co** (ESI) due to their four-fold symmetry.

Photochromism

The photocyclization/cycloreversion reactions of **1H₂**, **1Zn**, **1Ni** and **1Co** were followed by UV-visible absorption spectroscopy in dichloromethane under UV irradiation (ring closure reaction) and visible irradiation (ring-opening reaction). The photophysical data of the four porphyrins in their initial *open* state and at the photostationary state (PSS, after irradiation at 312 nm) together with their conversions (at PSS) determined by ¹H NMR are summarized in Table 1. Upon irradiation of a solution of **1H₂**, a broad band appeared in the visible region (500–700 nm), which is characteristic of the formation of *closed* DTE units (Figure 2, Table 1). Spectral changes were also observed in the UV part of the spectrum with a decrease of the absorption band at 290 nm and a concomitant increase of the absorption band around 360 nm. In addition, the absorption maximum of the Soret band diminished. Such a hypochromic feature was previously observed for related mono-DTE porphyrins and tentatively attributed to an effective electronic communication through a *p*-phenyl-acetylene linker.^[33] However, in the present work, the Soret band displays a broadening which can explain an apparent hypochromism in the absence of ground state electronic interactions. Under similar conditions, the electronic spectra of metallated porphyrins **1Zn**, **1Ni** and **1Co** display the characteristic low-energy absorption band at 500–700 nm, indicative of ring-closure processes (see

ESI). All photocyclization processes are reversible. Upon photoexcitation at 580 nm, the *closed* forms of all four compounds were converted back to their initial *open* forms and the electronic absorption spectra, notably the Soret band, were fully recovered in all cases (see ESI). A lack of electronic communication in the ground state between the four DTE units on each molecule is supported by the presence of distinct isosbestic points in the absorption spectra of all four compounds.^[14c,d] Finally, no degradation was observed after several irradiation cycles (UV \leftrightarrow visible), demonstrating the reversible photochromic behavior of these compounds.

Upon irradiation of a CD_2Cl_2 solution of **1H₂** at 300 nm, the ¹H NMR spectrum shows the characteristic upfield-shifted signals of the two thienyl protons of the *closed* DTEs at δ 6.85 and 6.65 ppm, (Figure 1, top) whereas the magnetically non-equivalent methyl protons appear as two singlets shifted downfield, at δ 2.36 and 2.23 ppm, compared to the methyl proton of the open DTEs (Figure S12). The signals of the *open*-DTE units are still present at the PSS, but it is not possible to discriminate between those of the initial *fully open* species (e.g. when all four DTE units on **1** are in the *open*-state) and the photo-generated *open-closed* derivatives. Therefore, in addition to the *fully-open* and *-closed tetra*-DTE-based porphyrin, the PSS is likely to contain a mixture of various isomers (o,o,o,c; o,o,c,c; o,c,o,c; o,c,c,c...), in which one, two, three or four DTE units are photocyclized. Moreover, a new low field singlet at δ 8.85 ppm is attributed to the β -pyrrolic protons of the photocyclized species.

The percentage of ring-closing in the photostationary state was determined by ¹H NMR spectroscopy (in CD_2Cl_2), by calculating the ratio of the integration between the thienyl signals of the *closed* DTE units and that of the β -pyrrolic protons, both in the *open* and PSS states. The photocyclization conversion was estimated to be 62, 88, and 75% for compounds **1H₂**, **1Zn** and **1Ni** respectively (Table 1). The higher conversion rate found for the metallated species could be explained by a ring-closure via the triplet state of *open*-DTE units, due to intersystem crossing.^[6,38] Notably, the efficiency at which these porphyrin-DTE scaffolds **1** photocyclize contrasts the reported inhibition of photoisomerization in several compounds in which porphyrins and the switching unit are linked by an ortho- or para-substituted phenyl spacer.^[22b,23,33,39] The *meta* substitution pattern in our edifices appears to limit efficiently the electronic delocalization in the molecular framework.

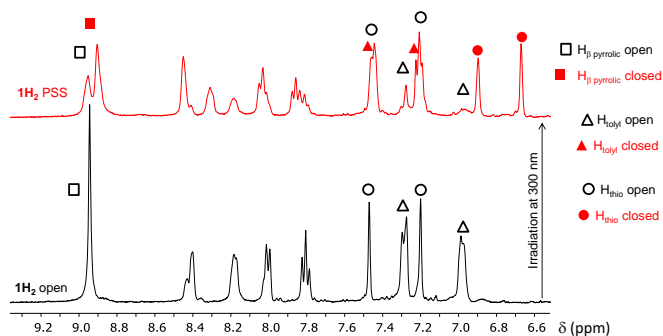


Figure 1. Partial ¹H NMR spectra (300 MHz, CD_2Cl_2) of **1H₂**; bottom: fully-open isomer, top: after irradiation with 300 nm light.

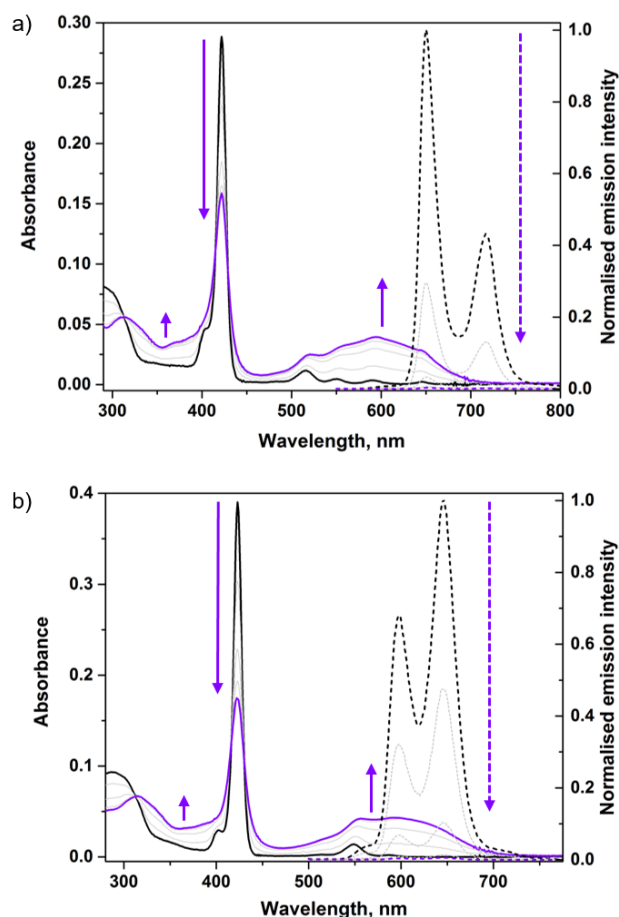


Figure 2. a) UV-visible absorption (solid line) and emission spectra (dashed line, $\lambda_{\text{exc}} = 429$ nm) of **1H₂** in CH_2Cl_2 (5×10^{-7} M) upon irradiation at 312 nm. b) UV-visible absorption (solid line) and emission spectra (dashed line, $\lambda_{\text{exc}} = 430$ nm) of **1Zn** in CH_2Cl_2 (5×10^{-7} M) upon irradiation at 312 nm.

Fluorescence properties of **1H₂** and **1Zn** – *open*-form

The emission spectra **1H₂** and **1Zn** measured at room temperature, in non-deaerated CH_2Cl_2 , exhibit features analogous to their counterparts without DTE units, namely the free base (H_2TPP) and the zinc-tetraphenylporphyrin^[40] (ZnTPP). The emission spectrum of **1H₂** displays two peaks, Q(0-0) and Q(0-1), respectively at 650 and 717 nm (Figure 2, Table 1 and ESI), whereas the excitation spectrum ($\lambda_{\text{em}} = 715$ nm) shows the same features as displayed by the absorption spectrum (see ESI). **1H₂** displays a fluorescence quantum yield $\Phi_F = 7.9 \pm 0.3\%$ in CH_2Cl_2 in the *open* form, which is in good agreement with the homologous, non-photochromic H_2TPP , for which $\Phi_F = 10\%$ in toluene.^[40] The lifetime for the radiative decay of S_1 of **1H₂** in the *open* form displays a monoexponential decay, with $\tau = 8.97 \pm 0.03$ ns ($\lambda_{\text{em}} = 650$ nm, $\lambda_{\text{exc}} = 590$ nm), in agreement with literature values for H_2TPP ($\tau = 12$ ns in benzene).^[41]

Interestingly, the metallated compound **1Zn** displays radiative deactivation from both $S_2 - S_0$, with a maximum at 426 nm, and $S_1 - S_0$, with two maxima at 597 and 646 nm for Q(0-0) and Q(0-1) respectively, in a fashion analogous to ZnTPP ^[42] (see ESI). The same considerations made for the excitation spectrum of **1H₂** are also valid for **1Zn** (see ESI). In the *open* form, **1Zn** displays a fluorescence quantum yield $\Phi_F = 4.8 \pm 0.2\%$ (for the $S_1 - S_0$ transition) in CH_2Cl_2 that is slightly higher, but still close to the homologous ZnTPP , showing $\Phi_F = 3.3\%$ in toluene.^[40]

Table 1. Photophysical properties of *open*-DTE and *closed*-DTE derivatives (PSS) of **1H₂**, **1Ni**, **1Zn** and **1Co** together with their photocyclization conversions

	λ_{\max} <i>open form</i> [nm] ($\epsilon \times 10^{-3}$ [M ⁻¹ cm ⁻¹]) ^[a]					λ_{\max} <i>closed form at PSS</i> [nm] ^[b]	λ_{em} <i>open form</i> [nm] ^[a]			Φ_F [%] ^[c]		% <i>Closed form at PSS</i> ^[d]	
	DTE	Soret (0-0)	Q _y (1-0)	Q _y (0-0)	Q _x (1-0)		Q _x (0-0)	S ₂ - S ₀	S ₁ - S ₀		<i>Open form</i>		PSS
									Q (0-0)	Q (0-1)			
1H₂	290 (160)	422 (580)	516 (24)	550 (9.4)	590 (7.1)	646 (4.4)	307, 593	650	717	7.9 ± 0.3	0.05 ± 0.01	62	
1Ni	285 (170)	417 (300)	527 (19)	553 (1.6)			310, 589					75	
1Zn	287 (190)	423 (780)	549 (28)	586 (4.2)			311, 592	426	597	646	4.8 ± 0.2	0.04 ± 0.02	88
1Co	290 (120)	414 (280)	529 (15)				312, 591					– ^[e]	

[a] 5×10^{-7} M in CH₂Cl₂, 298 K; [b] PSS attained under irradiation at $\lambda = 312$ nm. [c] Φ_F fluorescence quantum yield for the S₁ - S₀ transition of **1H₂** and **1Zn** in the open form and at the PSS (irr. 312 nm) determined by comparison with standard free base tetraphenylporphyrin (H₂TPP), for which Φ_F , R = 0.10 in toluene.^[40] [d] Determined by ¹H NMR. [e] Not determined by ¹H NMR due to the paramagnetic nature of the cobalt(II).

For **1Zn** in the *open* form, the lifetime of S₁ - S₀ emission showed a monoexponential decay, with $\tau = 1.9 \pm 0.1$ ns ($\lambda_{\text{em}} = 647$ nm, $\lambda_{\text{exc}} = 560$ nm), in agreement with literature values for ZnTPP ($\tau = 2$ ns in benzene).^[41]

Photoinduced modulation of **1H₂** and **1Zn** fluorescence

As a direct consequence of the photochromism of the DTE units covalently linked to the porphyrin core, for both the fluorescent **1H₂** and **1Zn** a quenching of their emission was noticed upon DTE closure triggered by UV light. Interestingly, the phenomenon was reversible, with the recovery of the original fluorescence upon visible ($490 \leq \lambda \leq 570$ nm) light irradiation, thus confirming the DTEs' role in the variation of the emission of **1H₂** and **1Zn**. The emission spectra (Figure 1 and ESI) were recorded upon excitation of the fluorophore in non-deaerated solutions in CH₂Cl₂ at one isosbestic point of the absorption spectra (429 and 430 nm for **1H₂** and **1Zn**, respectively) to rule out any variation of the emission spectra due to a change in the absorption of the excitation light upon DTE isomerization. Nevertheless, experiments performed at different excitation wavelengths showed the same phenomenon. Quenching of the fluorescence of the emissive free base porphyrin **1H₂** and the metallated **1Zn** was seen upon DTE ring closure (Figure 2). In addition, for **1Zn**, emission from S₂ ($\lambda_{\text{em}} = 426$ nm) was efficiently quenched upon DTE closure by UV irradiation (see ESI).

To assign the nature of the emissive species, excited state lifetime measurements were also performed upon DTE switching after UV irradiation. Upon partial switching of **1H₂** (short UV irradiation), the measurement showed a biexponential decay, with $\tau_1 = 9 \pm 2$ ns, and $\tau_2 = 7.7 \pm 0.8$ ns and relative amplitudes of 82% and 18%, respectively. Upon further switching (longer UV irradiation), the signal's intensity was too low to perform meaningful measurements. From these results, it seems evident that upon (short) irradiation a second species with shorter emission lifetime appears. This species could be a *partially closed*-DTE isomer that still emits light, but partial emission quenching is visible following its shorter lifetime. Upon increasing UV irradiation, the emission becomes so weak that no lifetime is measurable, which reflects a low concentration of the emissive species. Unfortunately, lifetime measurements on partially switched **1Zn** were not performed because, due to instrumental

limitations, the signal was too weak (nonoptimal excitation wavelength) to record.

At the PSS, attained upon UV light (312 nm) irradiation, **1H₂** and **1Zn** displayed luminescence quantum yields of $\Phi_F = 0.05 \pm 0.01\%$ and $\Phi_F = 0.04 \pm 0.02\%$, respectively. Here it is appropriate to state that the measurements were performed not on a single species, but most likely on a mixture of different, *partially closed* DTE isomers. Residual emission at the PSS (upon UV irradiation) therefore resulted from the presence of low concentrations of *all-open* and a *partially closed* isomer. This hypothesis is consistent with the low contrast in fluorescence intensity upon DTE photoswitching for similar reported compounds containing one or two DTE units.^[24,31] Overall, both compounds provided an excellent contrast between the emission spectra of the *all-open* and PSS states, mainly because of the presence of multiple quenchers around the fluorophore.

Multiple DTE switching cycles were performed and fluorescence intensity was recorded to explore the reversibility and resistance to fatigue of **1H₂** and **1Zn** (Figure 3). The intensity at the maximum of the fluorescence band was recorded at each irradiation step, upon excitation at the isosbestic point, as described earlier. **1H₂** showed almost complete reversibility, having recovered 85% of the initial emission intensity after 10 irradiation cycles in CH₂Cl₂, whereas **1Zn**, after the same number of cycles, displayed only 40% of the initial emission intensity. The latter is a clear indication of the lower photostability upon multiple irradiation cycles displayed by **1Zn** compared to its free base analogue. Nevertheless, the mechanism of photodegradation is still unknown and will be the subject of future investigations.

Photo-rewritable fluorescence patterning on **1H₂**-doped polystyrene films on glass

Fluorescence switching of the free base porphyrin **1H₂** was also performed on thin films of a blend of **1H₂** (8% in weight) and polystyrene (PS, average molecular weight = 500 kDa) spin-coated on glass substrates. The film on glass displayed absorption and emission spectra analogous to those shown by **1H₂** in its fully open form in CH₂Cl₂ solution (Figure 4). Moreover, photochromism of DTE and hence the photoswitchable fluorescence properties were retained, as observed in the emission spectra.

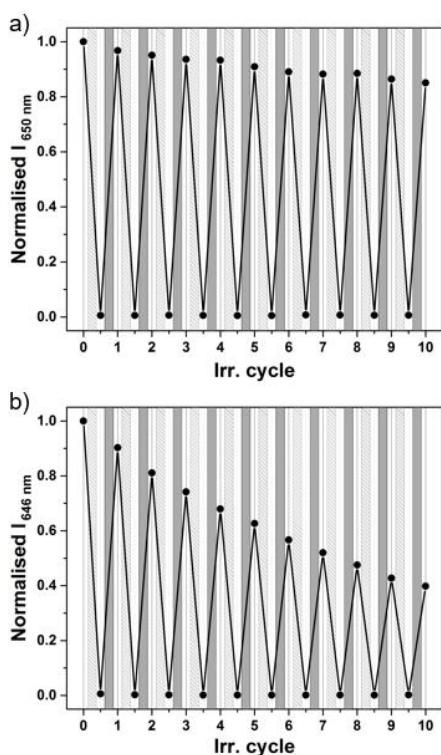


Figure 3. Variation of the emission intensity of a) **1H₂** and b) **1Zn** upon DTE isomerization by UV irradiation (light grey area, 312 nm; $t = 40$ s, $P_d = 3.0$ mW cm^{-2}) and subsequent ring opening by visible irradiation (dark grey area, green bandpass filter $\lambda_{\text{max}} = 530$ nm, FWHM = 80 nm; $t = 90$ s, $P_d @_{530 \text{ nm}} = 57.0$ mW cm^{-2}) in CH_2Cl_2 (5.0×10^{-7} M). Emission spectra were recorded in non-degassed CH_2Cl_2 solution ($c = 5.0 \times 10^{-7}$ M) upon excitation at 429 nm for **1H₂** and 430 nm for **1Zn**; the emission intensity was taken at the maximum of the fluorescence band (650 nm for **1H₂** and 646 nm for **1Zn**)

To understand the reversibility of the processes, multiple irradiation cycles were performed and showed the recovery of the initial emission intensity (Figure 4b). Nevertheless, due to limitations of the experimental setup, the data could only be used to show *qualitatively*^[43] that the photoswitching properties of **1H₂** were retained when the latter was dispersed into an amorphous polymer matrix and deposited as a thin film on a solid substrate.

Following the success in measuring the reversible fluorescence switching in films of **1H₂** with PS, we investigated the use of such a blend as a photoink for rewritable fluorescence patterning of thin films made on solid substrates. After deposition of the aforementioned blend as described earlier, positive and negative fluorescent patterns were recorded by structured illumination using a confocal laser scanning microscope (Figure 5). The reversible photoactivated luminescence quenching was exploited to record multiple patterns, by scanning with a UV laser (355 nm, 20 s scan) to trigger DTE ring-closure, therefore turning off the emission (dark areas, Figure 5), or with a visible laser (405 nm, 30 s scan) to trigger DTE ring-opening and to restore the original emission of the free-base porphyrin (bright areas, Figure 5). Based on the limitations of our instrumental set-up, the light source (visible laser, $\lambda = 405$ nm) employed for writing was also used for the luminescence read-out of the recorded patterns. Nevertheless, for imaging purposes, the use of lower laser power and scanning time sufficed to preserve the written information.

The successful demonstration of the utilization of the phototunable fluorescence properties of **1H₂** highlights its potential application as a photo-rewritable fluorescent ink for rewritable optical memory media or imaging purposes.

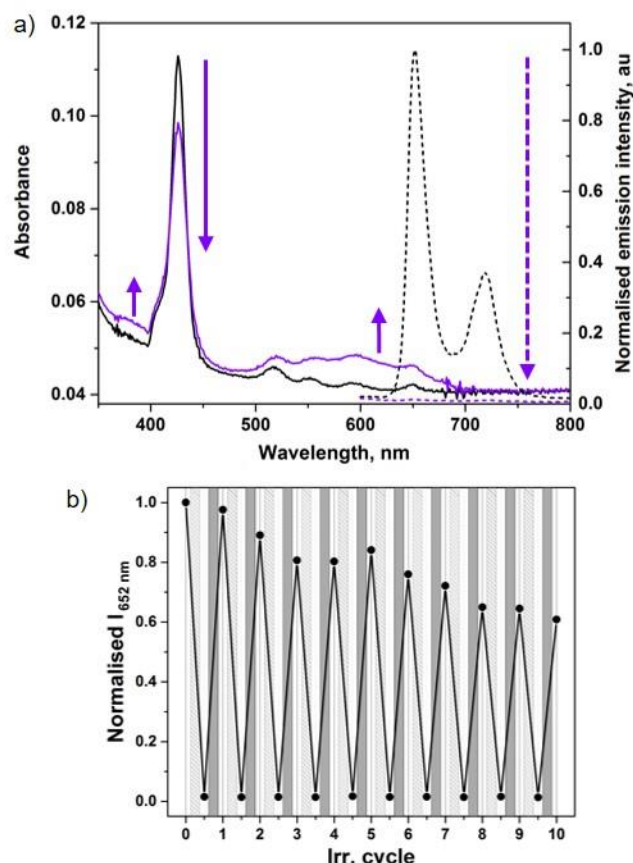


Figure 4. a) Absorption and emission spectra of **1H₂** in doped polystyrene film (500 kDa polystyrene, 8% w/w **1H₂**) spin-casted on glass upon DTE photocyclization by UV irradiation (312 nm; $P_d = 3.0$ mW cm^{-2}). b) Variation of the emission intensity of **1H₂** upon alternated UV irradiation (light grey area, 312 nm) and visible irradiation (dark grey area, green bandpass filter $\lambda_{\text{max}} = 530$ nm, FWHM = 80 nm) in a doped polystyrene film (500 kDa polystyrene, 8% w/w **1H₂**) spin-casted on glass.

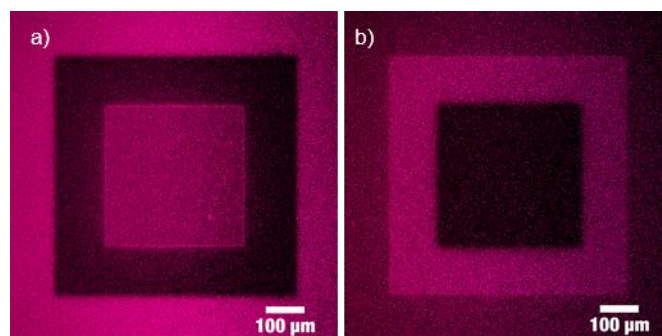


Figure 5. Confocal laser scanning microscope images taken on **1H₂**-doped polystyrene film (500 kDa polystyrene, 8% w/w **1H₂**) spin-casted on glass. The film was selectively patterned upon subsequent UV or visible laser irradiation by scanning on three square-shaped areas and progressively decreasing the scan size. a) Vis light (405 nm laser, 3% power, 30 s), UV light (355 nm laser, 20 s) and Vis light. b) UV light, visible light and UV light. Imaging was performed upon excitation of **1H₂** at $\lambda_{\text{exc}} = 405$ nm (0.5% power, 1.7 s per frame), collecting emission $414 \leq \lambda_{\text{em}} \leq 721$ nm light

Conclusions

The efficient and reversible photoisomerization observed in a family of novel tetra-dithienylethene-substituted porphyrins demonstrates that a high density of functional switching units can be arranged around a porphyrin framework by covalent linkage via a *meta*-phenyl spacer. The tetra-DTE-porphyrin arrays **1H₂** and **1Zn** displayed reversible luminescence switching properties, due to the quenching of the singlet emissive state of the luminophore by intramolecular energy transfer to the *closed* form of DTE. Upon DTE photoswitching, a nearly complete quenching of the porphyrin's fluorescence was attained, providing a highly contrasted readout of the switching event. In addition to their photoregulated fluorescence, the possibility to trigger the switch and detect the output at very distinct wavelengths renders these systems of interest for applications in optical devices. Moreover, the applicability of **1H₂** as a photo-rewritable fluorescent ink was demonstrated, opening perspectives towards its application in all-optical memory storage and fluorescence microscopy imaging.

Experimental Section

UV-visible absorption spectroscopy. UV-visible absorption spectroscopy experiments on **1Co** in solution required a degassing procedure on a high-vacuum line in a degassing cell, which consists of a 10-mL Pyrex bulb and a 1-cm path length quartz cuvette, sealed from the atmosphere by a Teflon stopper. Three successive freeze-pump-thaw cycles were performed to degas the solution. For photoisomerization experiments followed by UV-visible absorption spectroscopy of compounds **1H₂**, **1Zn** and **1Ni**, the solutions were not degassed and a 1 cm quartz cell was used. Photoisomerization in solution was performed with an LS series Light Source of ABET technologies, Inc (150 W xenon lamp), with single wavelength light filters "320FS 10-25" for ring-closure and "580FS 10-25" for cycloreversion. Alternatively, photoisomerisation studies were performed with a Herolab UV 6ML 312 nm lamp, at an incident power density $P_d = 3.0 \text{ mW cm}^{-2}$ for DTE electrocyclization reaction. Visible light irradiation was carried out using an Edmund Optics illuminator equipped with a 150 W halogen lamp and a green filter ($\lambda_{\text{max}} = 530 \text{ nm}$, FWHM = 80 nm) at an incident power density $P_{d, 530 \text{ nm}} = 57 \text{ mW cm}^{-2}$, for DTE cycloreversion. During light irradiation, the solutions were always vigorously stirred. Irradiation for ¹H NMR experiments was carried out using a Rayonet® with 300 nm light emitting lamps.

Fluorescence. All the photophysical studies were performed in spectroscopy grade dichloromethane (Sigma Aldrich), using 1 cm or 3 mm optical path length Suprasil quartz cuvettes (Hellma). Except for lifetime measurements, the studies were performed at low concentration ($c = 5.0 \cdot 10^{-7} \text{ M}$), to keep the absorbance at the excitation wavelength lower than 0.1 in order to avoid reabsorption of the emitted light. Emission spectra were recorded with an Agilent Cary Eclipse and a Horiba Jobin Yvon Fluorolog FL3-22 fluorometers. Lifetime measurements were performed by single photon counting with a Horiba Jobin Yvon Fluorolog FL3-22 fluorometer equipped with a FluoroHub A+ TCSPC controller and a PPD picosecond single-photon counting detector. Excitation was performed using NanoLED LED light sources (pulse width $\leq 1.3 \text{ ns}$), using $\lambda_{\text{exc}} = 590 \text{ nm}$ for **1H₂** and $\lambda_{\text{exc}} = 560 \text{ nm}$ for **1Zn**. Following the short lifetime of **1Zn**, the excitation pulse profile was deconvoluted by measuring the instrument response function using a scattering dispersion of colloidal silica (Ludox - Sigma Aldrich) in water. Quantum yield measurements were carried out by comparison with a standard compound with known quantum yield. For the purpose, free base tetraphenylporphyrin (H₂TTPP, Sigma Aldrich) in toluene was used, which has $\Phi_{F,R} = 0.10$.^[39] The measurements were performed upon excitation of **1H₂** and **1Zn** at the isosbestic points (429 and 430 nm respectively) of their absorption spectra upon DTE

isomerization, in order to rule out any change in the absorption of the excitation light. Concentration was kept low, in order to have $A_{\lambda_{\text{exc}}} \leq 0.05$.

1H₂ – polystyrene films. **1H₂** was deposited on solid substrates upon blending with high-molecular weight polystyrene (PS, average: 500 kDa, Sigma Aldrich, low polydispersity, standard for GPC) in 8% weight ratio. The solutions were prepared at a PS concentration of 3 mg mL⁻¹ in CHCl₃ and deposited on glass by spin-coating. The glass slides (standard microscope slides) were washed following standard cleaning procedure by rinsing with acetone, isopropanol, ethanol and blown with nitrogen, no further surface treatment was performed. The films were characterized by optical microscope and surface profiler, they showed uniform surface coverage and an average thickness of ~20 nm. The photophysical properties of the as-deposited films were measured with a Jasco V-650 spectrophotometer equipped with solid sample holder, and with an Agilent Cary Eclipse fluorometer equipped with a movable solid sample holder, holding the sample in right-angle excitation geometry.

Confocal laser imaging. Fluorescence confocal images were recorded by using a Zeiss LSM 710 confocal microscope system with a 10× magnification objective. Imaging was performed upon exciting the samples with a continuous wave laser at $\lambda_{\text{exc}} = 405 \text{ nm}$, 1.7 s per frame, 0.3% power. The emission of the assemblies was collected in the range from 414 to 721 nm by using the lambda-mode option. The raw data recorded by means of the lambda-mode were processed by using linear un-mixing tool option available in the ZEN 2011 software package (Zeiss GmbH, Germany). In order to turn off **1H₂** fluorescence a UV continuous wave laser was used ($\lambda = 355 \text{ nm}$), by scanning on the same frame for 20 seconds, while to turn on **1H₂** fluorescence the same $\lambda = 405 \text{ nm}$ laser for imaging was used, but at higher power, scanning on the frame for 30 seconds.

Synthesis of 4. *n*Butyl lithium (1.6 M in hexane, 1.2 mL, 1.9 mmol) was slowly added to a solution of bromothiophene **2** (566 mg, 1.74 mmol) in dry THF (20 mL) at -78 °C under argon. After 30 min, a solution of 2-methyl-3-(perfluorocyclopent-1-en-1-yl)-5-(*p*-tolyl)thio-phenone **3** (662 mg, 1.74 mmol) in dry THF was added and the resulting mixture was allowed to warm to r.t. and stirred for 15 h. HCl (0.5 M, 10 mL) was then added and the mixture was stirred for 30 min. The solvents were removed in vacuum. The residue was extracted with CH₂Cl₂ and washed with saturated NaHCO_{3(aq)}. The combined organic phases were then dried, filtered and evaporated to give a thick brown oil as the crude product. Purification by chromatography over silica gel (cyclohexane/CH₂Cl₂ (4/1)) afforded **4** as a yellowish paste (440 mg, 782 μmol, 45%). ¹H NMR (300 MHz, CDCl₃): δ ppm = 10.05 (s, 1H), 8.03 (t, $J = 1.6 \text{ Hz}$, 1H), 7.80 (m, 2H), 7.56 (t, $J = 7.7 \text{ Hz}$, 1H), 7.43 (dd, $J = 6.4$; 1.8 Hz, 2H), 7.37 (s, 1H), 7.22 (s, 1H), 7.19 (dd, $J = 6.4$; 1.8 Hz, 2H), 2.37 (s, 3H), 1.99 (s, 3H), 1.97 (s, 3H). ¹³C NMR (75 MHz, CDCl₃): δ ppm = 14.69, 14.76, 21.34, 121.92, 123.65, 125.72, 125.79, 126.33, 126.39, 129.29, 129.83, 129.92, 130.65, 131.39, 134.53, 137.18, 138.13, 140.66, 140.85, 142.45, 142.70, 192.01. ¹⁹F (282 MHz, CDCl₃): δ ppm = -110.9, -111.1, -132.9. HRMS for C₁₃₂H₈₆F₂₄N₄S₈⁺ calc.: $m/z = 2439.4308$; found: $m/z = 2439.4356$. HRMS for [C₂₉H₂₆F₆O₁S₂ + Na]⁺ calc.: $m/z = 585.0752$; found: $m/z = 585.0740$.

Synthesis of 1H₂. To a degassed solution of **10** (341 mg, 584 μmol) and pyrrole (40 μL, 584 μmol) in CH₂Cl₂ (58 mL) and ethanol (0.44 mL) was added BF₃·OEt₂ (1 M, 0.19 mL). After 1 h, *p*-chloranil (107 mg) was added to the solution. After 1 h, solvents were removed under vacuum. Chromatography over silica (cyclohexane/CH₂Cl₂ (3/2)) afforded **1H₂** as purple powder (118 mg, 48 μmol, 32%). ¹H NMR (300 MHz, CDCl₃): δ ppm = 8.99 (s, 8H), 8.45 (s, 4H), 8.22 (d, $J = 7.4 \text{ Hz}$, 4H), 8.03 (dt, $J = 7.8 \text{ Hz}$; 1.3 Hz, 4H), 7.82 (t, $J = 7.3 \text{ Hz}$, 4H), 7.53 (s, 4H), 7.36 (d, $J = 7.9 \text{ Hz}$, 8H), 7.25 (s, 4H), 7.06 (d, $J = 7.9 \text{ Hz}$, 8H), 2.28 (s, 12H), 2.06 (s, 12H), 2.03 (s, 12H), -2.65 (s, 2H). ¹³C NMR (125 MHz, CDCl₃): δ ppm = 14.68, 21.12, 26.95, 29.76, 34.84, 34.97, 96.15, 119.61, 121.83, 123.14, 125.01, 125.47, 125.72, 126.22, 127.49, 129.58, 130.49, 131.47, 131.56, 131.87, 134.03, 137.84, 140.78, 141.86, 142.43, 142.90. ¹⁹F (282 MHz, CDCl₃): δ ppm = -110.9, -111.1, -132.9. UV-Vis (CH₂Cl₂, 298 K): λ (nm) [ϵ (M⁻¹.cm⁻¹)] 291

[130,000], 422 [530,000], 517 [21,000], 551 [8,200], 590 [6,300], 646 [3,900]. HRMS for $C_{132}H_{84}F_{24}N_4S_8^+$ calc.: $m/z = 2439.4308$; found: $m/z = 2439.4356$.

Synthesis of 1Zn. A solution of **1H₂** (50 mg, 21 μ mol) and Zn(OAc)₂•2H₂O (23 mg, 105 μ mol) in MeOH (0.22 mL) and CHCl₃ (2.2 mL) was stirred for 45 min at r.t. Solvents were removed under vacuum. Chromatography over silica (CH₂Cl₂) afforded **1Zn** as a dark purple powder (50 mg, 20 μ mol, 95%). ¹H NMR (300 MHz, CDCl₃): δ ppm = 9.03 (s, 8H), 8.40 (s, 4H), 8.16 (d, $J = 7.6$ Hz, 4H), 7.98 (d, $J = 7.6$ Hz, 4H), 7.78 (t, $J = 7.6$ Hz, 4H), 7.45 (s, 4H), 7.31 (d, $J = 7.9$ Hz, 8H), 7.18 (s, 4H), 7.03 (m, 8H), 2.23 (s, 12H), 2.00 (s, 12H), 1.98 (s, 12H). UV-Vis (CH₂Cl₂, 298 K): ϵ (nm) [ϵ (M⁻¹.cm⁻¹)] 290 [130,000], 424 [580,000], 549 [23,000], 586 [4,100]. HRMS for [C₁₃₂H₈₄F₂₄N₄S₈Zn+Na]⁺ calc.: $m/z = 2523.3262$; found: $m/z = 2523.3192$.

Synthesis of 1Ni. A solution of **1H₂** (50 mg, 21 μ mol) and Ni(acac)₂ (7 mg, 26 μ mol) in PhCl (1 mL) was refluxed for 45 min. After cooling to r.t., chromatography over silica (CH₂Cl₂) afforded **1Ni** as a red powder (50 mg, 20 μ mol, 96%). ¹H NMR (300 MHz, CDCl₃): δ ppm = 8.85 (s, 8H), 8.20 (s, 4H), 8.00 (d, $J = 7.7$ Hz, 4H), 7.92 (d, $J = 7.7$ Hz, 4H), 7.73 (t, $J = 7.7$ Hz, 4H), 7.44 (s, 4H), 7.37 (d, $J = 8.1$ Hz, 8H), 7.21 (s, 4H), 7.09 (d, $J = 8.1$ Hz, 8H), 2.29 (s, 12H), 2.00 (s, 12H), 1.97 (s, 12H). UV-Vis (CH₂Cl₂, 298 K): λ (nm) [ϵ (M⁻¹.cm⁻¹)] 292 [110,000], 418 [240,000], 528 [17,000], 553 [5,100]. HRMS for C₁₃₂H₈₄F₂₄N₄NiS₈⁺ calc.: $m/z = 2494.3426$; found: $m/z = 2494.3609$.

Synthesis of 1Co. A solution of **1H₂** (50 mg, 21 μ mol) and Co(OAc)₂•4H₂O (42 mg, 168 μ mol) in MeOH (1 mL) and CHCl₃ (2 mL) was refluxed for 1 h. After cooling to r.t., solvents were removed under vacuum. The residue was dissolved in CH₂Cl₂ (5 mL) and washed with H₂O (2 x 5 mL). The organic layer was reduced under vacuum. Chromatography over silica (cyclohexane/CH₂Cl₂ (5/1)) afforded **1Co** as a red powder (49 mg, 19 μ mol, 93%). HRMS for C₁₃₂H₈₄CoF₂₄N₄S₈⁺ calc.: $m/z = 2495.3405$; found: $m/z = 2495.3445$. UV-Vis (CH₂Cl₂, 298 K): λ (nm) [ϵ (M⁻¹.cm⁻¹)] 290 [120,000], 414 [280,000], 529 [15,000].

Acknowledgements

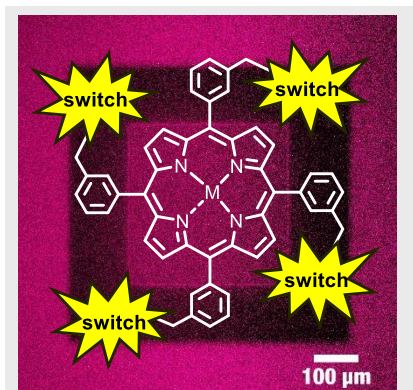
This work was supported by the Agence Nationale de la Recherche through the Labex projects CSC (ANR-10-LABX-0026 CSC) within the Investissement d'Avenir program (ANR-10-120 IDEX-0002-02), by the International Center for Frontier Research in Chemistry (JWe-CSC-0001), by the Université de Strasbourg, the Centre National de la Recherche Scientifique and the Université de Rennes as well as by the European Commission through the Marie Skłodowska-Curie project ITN project iSwitch (GA-642196). We gratefully acknowledge Dr. Sara Bonacchi and Marco A. Squillaci for enlightening discussions, and Dr. Alessandro Aliprandi for the confocal laser scanning microscope images.

Keywords: photochromism • dithienylethene • porphyrinoids • fluorescence • photopatterning

- [1] (a) M. M. Russew, S. Hecht, *Adv. Mater.* **2010**, *22*, 3348-3360; (b) X. Zhang, L. Hou, P. Samori, *Nat. Commun.*, **2016**, *7*, 11118.
- [2] (a) M. Irie, *Chem. Rev.* **2000**, *100*, 1685-1716; (b) H. Tian, S. Yang, *Chem. Soc. Rev.* **2004**, *33*, 85-97; (c) M. Irie, T. Fukaminato, K. Matsuda, S. Kobatake, *Chem. Rev.* **2014**, *114*, 12174-12277.
- [3] (a) E. Orgiu, N. Crivillers, M. Herder, L. Grubert, M. Pätzelt, J. Frisch, E. Pavlica, G. Bratina, N. Koch, S. Hecht, P. Samori, *Nat. Chem.* **2012**, *4*, 675-679; (b) T. Mosciatti, M. G. del Rosso, M. Herder, J. Frisch, N. Koch, S. Hecht, E. Orgiu, P. Samori, *Adv. Mater.*, **2016**, *28*, 6606-6611.
- [4] E. Orgiu, P. Samori, *Adv. Mater.* **2014**, *26*, 1827-1845.
- [5] For selected examples of photochromic modulation of fluorescence, see G. M. Tsivgoulis, J.-M. Lehn, *Angew. Chem. Int. Ed.* **1995**, *34*, 1119-1122; (b) A. Fernandez-Acebes, J. M. Lehn, *Chem. Eur. J.* **1999**, *5*, 3285-3292; (c) T. Kawai, T. Sasaki, M. Irie, *Chem. Commun.* **2001**, 711-712; (d) M. Irie, T. Fukaminato, T. Sasaki, N. Tamai, T. Kawai, *Nature*, **2002**, *420*, 759-760; (e) T. Fukaminato, T. Sasaki, T. Kawai, N. Tamai, M. Irie, *J. Am. Chem. Soc.* **2004**, *126*, 14843; (f) T. Fukaminato, *J. Photochem. Photobiol. C*, **2011**, *12*, 177-208; (g) J. X. Liu, B. Xin, C. Li, N.-H. Xie, W.-L. Gong, Z.-L. Huang, M.-Q. Zhu, *ACS Appl. Mater. Interfaces*, **2017**, *9*, 10338-10343.
- [6] (a) V. Guerschais, J. Boixel, H. Le Bozec, In *Photon-Working Switches*, (Eds. Y. Yokoyama, K. Nakatani) Springer Japan, 2017, Chapter 18; (b) V. Guerschais, L. Ordonneau, H. Le Bozec, *Coord. Chem. Rev.* **2010**, *254*, 2533-2545.
- [7] (a) A. Kronemeijer, H. B. Akkerman, T. Kudernac, B. J. van Wees, B. L. Feringa, P. W. M. Blom, B. de Boer, *Adv. Mater.* **2008**, *20*, 1467-1473; (b) S. J. van der Molen, J. Liao, T. Kudernac, J. S. Agustsson, L. Bernard, M. Calame, B. J. van Wees, B. L. Feringa, C. Schönenberger, *Nano Lett.* **2009**, *9*, 76-80; (c) F. Meng, Y.-M. Hervault, L. Norel, K. Costuas, C. Van Dyck, V. Geskin, J. Cornil, H. Hoon Hng, S. Rigaut, X. Chen, *Chem. Sci.* **2012**, *3*, 3113-3118; (d) C. Jia, A. Migliore, N. Xin, S. Huang, J. Wang, Q. Yang, S. Wang, H. Chen, D. Wang, B. Feng, Z. Liu, G. Zhang, D.-H. Qu, H. Tian, M.-A. Ratner, H.-Q. Xu, A. Nitzan, X. Guo, *Science*, **2016**, *352*, 1443-1445.
- [8] (a) J. J. D. de Jong, L. N. Lucas, R. M. Kellogg, J. H. van Esch, B. L. Feringa, *Science*, **2004**, *304*, 278-281; (b) J. T. Van Herpt, M. C. A. Stuart, W. R. Browne, B. L. Feringa, *Chem. Eur. J.* **2014**, *20*, 3077-3083.
- [9] (a) U. Al-Atar, R. Fernandes, B. Johnsen, D. Baillie, N. R. Branda, *J. Am. Chem. Soc.* **2009**, *131*, 15966-15967; (b) O. Yehezkeili, M. Moshe, R. Tel-Vered, Y. Feng, Y. Li, H. Tian, J. Willner, *Analyst*, **2010**, *135*, 474-476.
- [10] T. Leydecker, M. Herder, E. Pavlica, G. Bratina, S. Hecht, E. Orgiu, P. Samori, *Nat. Nanotech.*, **2016**, *11*, 769-775.
- [11] Two DTEs linked by a silyl spacer: J. Areephong, W. R. Browne, B. L. Feringa, *Org. Biomol. Chem.* **2007**, *5*, 1170-1174.
- [12] C. Li, H. Yan, L.-X. Zhao, G.-F. Zhang, Z. Hu, Z.-L. Huang, M.-Q. Zhu, *Nat. Commun.* **2014**, *5*, 5709.
- [13] J. Areephong, H. Logtenberg, W. R. Browne, B. L. Feringa, *Org. Lett.* **2010**, *12*, 2132-2135.
- [14] Arenyl spacers: H. Choi, H. Jung, K. H. Song, D.-S. Shin, S. O. Kang, J. Ko, *Tetrahedron*, **2006**, *62*, 9059-9065.
- [15] (a) A. Fihey, A. Perrier, W. R. Browne, D. Jacquemin, *Chem. Soc. Rev.* **2015**, *44*, 3719-3759; (b) A. Perrier, F. Maurel, D. Jacquemin, *Acc. Chem. Res.* **2012**, *45*, 1173-1182; (c) D. Bleger, J. Dokic, M. V. Peters, L. Grubert, P. Saalfrank, S. Hecht, *J. Phys. Chem. B*, **2011**, *115*, 9930-9940; (d) F. Cisnetti, R. Ballardini, A. Credi, M. T. Gandolfi, S. Masiero, F. Negri, S. Pieraccini, G. P. Spada, *Chem. Eur. J.* **2004**, *10*, 2011-2021.
- [16] H. Tian, B. Chen, H. Tu, K. Müllen, *Adv. Mater.* **2002**, *14*, 918-923.
- [17] DTEs bridged by an alkynyl spacer: T. Kaieda, S. Kobatake, H. Miyasaka, M. Murakami, N. Iwai, Y. Nagata, A. Itaya, M. Irie, *J. Am. Chem. Soc.*, **2002**, *124*, 2015-2014.
- [18] Alkyl spacers: (a) A. Peter, N. R. Branda, *Adv. Mater. Opt. Electron.* **2000**, *10*, 245-249; (b) T. Kaieda, S. Kobatake, H. Miyasaka, M. Murakami, N. Iwai, Y. Nagata, A. Itaya, M. Irie, *J. Am. Chem. Soc.* **2002**, *124*, 2015-2024.
- [19] Alkynyl spacer: K. Yagi, M. Irie, *Chem. Lett.* **2003**, *32*, 848-849.
- [20] Arenyl spacers: T. Kawai, T. Sasaki, M. Irie, *Chem. Commun.*, **2001**, 711-712.
- [21] DTEs arranged around metal complexes: (a) E. C. Harvey, B. L. Feringa, J. G. Vos, W. R. Browne, M. T. Pryce, *Coord. Chem. Rev.* **2015**, *282*, 77-86; (b) L. Ordonneau, V. Aubert, V. Guerschais, A. Boucekkinne, H. Le Bozec, A. Singh, I. Ledoux, D. Jacquemin, *Chem. Eur. J.*, **2013**, *19*, 5845-5849.
- [22] (a) D. R. Reddy, B. G. Maiya, *Chem. Commun.* **2001**, 117-118; (b) D. R. Reddy, B. G. Maiya, *J. Phys. Chem. A*, **2003**, *107*, 6326-6333; (c) M. V. Peters, R. Goddard, S. Hecht, *J. Org. Chem.* **2006**, *71*, 7846-7849.
- [23] C. A. Hunter, L. D. Sarson, *Tetrahedron Lett.* **1996**, *37*, 699-702.

- [24] H. J. Kim, J. H. Jang, H. Choi, T. Lee, J. Ko, M. Yoon, H.-J. Kim, *Inorg. Chem.* **2008**, *47*, 2411-2415.
- [25] J. Frey, G. Kodis, S. D. Straight, T. A. Moore, A. L. Moore, D. Gust, *J. Phys. Chem. A*, **2013**, *117*, 607-615.
- [26] P. A. Liddell, G. Kodis, A. L. Moore, T. A. Moore, D. Gust, *J. Am. Chem. Soc.* **2002**, *124*, 7668-7669.
- [27] D. E. Williams, J. A. Rietman, J. M. Maier, R. Tan, A. B. Greytak, M. D. Smith, J. A. Krause, N. B. Shustova, *J. Am. Chem. Soc.* **2014**, *136*, 11886-11889.
- [28] L. Hou, X. Zhang, T. C. Pijper, W. R. Browne, B. L. Feringa, *J. Am. Chem. Soc.* **2014**, *136*, 910-913.
- [29] O. Nevskiy, D. Sysoiev, A. Oppermann, T. Huhn, D. Woll, *Angew. Chem. Int. Ed.* **2016**, *55*, 12698-12702.
- [30] B. Roubinet, M. L. Bossi, P. Alt, M. Leutenegger, H. Shojaei, S. Schnorrenberg, S.; Nizamov, M. Irie, V. N. Belov and S. W. Hell, *Angew. Chem. Int. Ed.* **2016**, *55*, 15429-15433.
- [31] B. Roubinet, M. Weber, H. Shojaei, M. Bates, M. L. Bossi, V. N. Belov, M. Irie, S. W. Hell, *J. Am. Chem. Soc.* **2017**, *139*, 6611-6620.
- [32] (a) T. B. Norsten, N. R. Branda, *J. Am. Chem. Soc.*, **2001**, *123*, 1784-1785; (b) J. Kärnbratt, M. Hammarson, S. Li, H. L. Anderson, B. Albinsson, J. Andréasson, *Angew. Chem. Int. Ed.* **2010**, *49*, 1854-1857; (c) T. B. Norsten, N. R. Branda, *Adv. Mater.* **2001**, *13*, 347-349.
- [33] A. Osuka, D. Fujikane, H. Shinmori, S. Kobatake and M. Irie, *J. Org. Chem.* **2001**, *66*, 3913-3923.
- [34] S. D. Straight, P. A. Liddell, Y. Terazono, T. A. Moore, A. L. Moore, D. Gust, *Adv. Funct. Mater.* **2007**, *17*, 777-785.
- [35] (a) J. S. Lindsey, H. C. Hsu and I. C. Schreiman, *Tetrahedron Lett.* **1986**, *27*, 4969-4970; (b) J. S. Lindsey, I. C. Schreiman, H. C. Hsu, P. C. Kearney, A. M. Marguerettaz, *J. Org. Chem.* **1987**, *52*, 827-836.
- [36] S. Yamamoto, K. Matsuda, M. Irie, *Angew. Chem. Int. Ed.* **2003**, *42*, 1636-1639.
- [37] S. Pu, L. Hui, L. Gang, L. Weijun, C. Shiqiang, F. Congbin, *Tetrahedron*, **2011**, *67*, 1438-1447.
- [38] E. G. Azenha, A. C. Serra, M. Pineiro, M. M. Pereira, J. Seixas de Melo, L. G. Arnaut, S. J. Fromosinho, A. M. d'A. Rocha Gonsalves, *Chem. Phys.* **2002**, *280*, 177-190.
- [39] A. J. Myles, N. R. Branda, *Tetrahedron Lett.* **2000**, *41*, 3785-3788.
- [40] M. Pineiro, A. L. Carvalho, M. M. Pereira, A. M. Rocha Gonsalves, L. G. Arnaut, S. Formosinho, *J. Chem. Eur. J.*, **1998**, *4*, 2299-2307.
- [41] J. S. Baskin, H.-Z. Yu and A. H. Zewail, *J. Phys. Chem. A* **2002**, *106*, 9837-9844.
- [42] H.-Z. Yu, J. S. Baskin and A. H. Zewail, *J. Phys. Chem. A* **2002**, *106*, 9845-9854.
- [43] In the experimental set-up used, emission on thin films was measured with a standard right-angle excitation optical scheme. Conversely, to perform quantitative measurements, the use of an integrating sphere would be necessary. See also: H. Ishida, J.-C. Bünzli, A. Beeby, *Pure Appl. Chem.* **2016**, *88*, 701-711,

Think pink ink. Multiple switching events of dithienylethenes around a porphyrin core provide highly contrasted fluorescence readout and photo-rewritable fluorescent inks.



*T. Biellmann, A. Galanti, J. Boixel
J. A. Wytko, V. Guerschais, * P.
Samori* and Jean Weiss **

Page No. – Page No.

**Fluorescence commutation and
surface photopatterning with
porphyrin tetra-dithienylethene
switches**